Electronic Supplementary Material (ESI) for ChemComm.

Facile Synthesis of NHC-stabilized Ni Nanoparticles and their Catalytic Application in the Z-selective Hydrogenation of Alkynes

M. Díaz de los Bernardos[a], S. Pérez-Rodríguez[a], A. Gual[a], C. Godard[a,b] and C. Claver[a,b]

[a]*Centre Tecnològic de la Química de Catalunya (CTQC), 43007 Tarragona, Spain*
[b]*Departament de Química Física i Inorgànica, Facultat de Química, Universitat Rovira i Virgili, 43007, Tarragona, Spain*

Table of contents:

S1. Reagents, general methods and characterization techniques

S2. Synthesis of the imidazoliumm carboxilate

S3. Synthesis of colloidal and CNT-supported Ni nanoparticles

S4. Characterization of the colloidal Ni nanoparticles

S5. Validation of the procedure

S6. Characterization of the CNT-supported Ni nanoparticles

S7. References

S1. Reagents, general methods and characterization techniques

S1.1. Reagents and general methods

All syntheses were performed using standard Schlenck techniques under N_2 or Ar atmosphere. Chemicals were purchased from Aldrich Chemical Co and Stream. All solvents were distilled over drying reagents and were deoxygenated before use. The syntheses of the nanoparticles were performed using 1L Fisher Porter and pressurized on a high pressure line. Air sensitive reactions were carried out under argon in dry solvents and glassware. Flash column chromatography was carried out using a forced flow of the indicated solvent on Merck silica gel 60 (230−400 mesh). Reactions were monitored by TLC carried out on 0.25 mm E. Merck silica gel 60 F_{254} glass or aluminum plates.

S1.2. Characterization techniques

Transmission electron microscopy (TEM) experiments were performed at the "Unitat de Microscopia dels Serveis Cientificotècnics de la Universitat Rovira I Virgili" (TEM-SCAN) in Tarragona with a Zeis 10 CA electron microscope operating at 100 kV with resolution of 3Å. The particles size distributions were determined by a manual analysis of enlarged images. At least 300 particles on a given grid were measured in order to obtain a statistical size distribution and a mean diameter.

High resolution transmission electron microscopy (HR-TEM) and scanning transmission electron microscopy (STEM) micrographs were obtained using a Tecnai F30 (300 kV) equipped with a STEM module and a high-angle annular dark-field detector, available in the "Advanced Microscopy Laboratory of Instituto de Nanociencia de Aragón" in Zaragoza. The samples were dispersed in THF and a small amount (around 3-5 drops) of solution was then deposited on a Cu-carbon grid.

X-ray diffraction (XRD) measurements were made using a Siemens D5000 diffractometer (Bragg-Brentano parafocusing geometry and vertical θ-θ goniometer) fitted with a curved graphite diffracted beam monochromator, incident and diffracted-beam Soller slits, a 0.06° receiving slit and scintillation counter as a detector. The angular 2θ diffraction range was between 20 and 95°. The data were collected with an angular step of 0.05° at 6s per step and sample rotation. A low background Si(510) wafer was used as sample holder. $Cu_{k\alpha}$ radiation was obtained from a copper Xray tube operated at 40kV and 30 mA. Crystallite sizes for metal or metal oxides nanoparticles of Ni were calculated from adjusting the respective diffraction line (considering all the peaks) to a pseudo-Voigt function by means of the Pawley-LeBail method and refining the cell parameters, using the Scherrer's equation and the software TOPAS which allows a proper deconvolution of the signals associated to carbon and metal nanoparticles. The peak width was obtained from the integral breadth (IB) which is equivalent to the width of a rectangle with the same area and peak height than the studied peak assuming K = 1.[1]

X-ray photoelectron spectroscopy (XPS) analyses were performed in an ESCAPlus OMICRON system equipped with a hemispherical electron energy analyser. The spectrometer operated at 225 W (15 mA, 15 kV), using a MgKα (1253.6 eV) anode and under vacuum ($<5 \cdot 10^{-9}$) using an analysis area of 1.75×2.75 mm. A survey scan (1sweep/200 ms dwell) was acquired between 0 and 1000 eV, at 0.5 eV step, 0.2 s dwell and 50 eV pass energy. High resolution scans for C 1s, O 1s and Ni 2p were obtained at 0.1 eV step, 0.5 s dwell and 20 eV pass energy. Binding energies were calibrated relative to the C 1s photoemission at 284.5. The XPS data were curve-resolved using the CASAXPS software after Shirley background subtraction. The spectra were fit with the minimum number of peaks needed to reproduce the spectral features. Gaussian (70%)–Lorentzian (30%), defined in CasaXPS as GL(30)[2], profiles were used for each component, with the exception of the metallic nickel contribution. In this case an asymetric peak shape defined by standard nickel metal sample, CasaXPS peak shape parameter = A(0.4,0.55,10)GL (30).[3] Samples were analyzed after sputtering with a 500 eV argon ion beam during 300s to further investigate the surface composition of Ni nanoparticles.

Thermogravimetric analysis (TGA) was carried out using a Mettler Toledo TGA/DSC 1 microbalance. Analyses were performed in air (20 NmL min^{-1}) or N_2 (20 NmL min^{-1}) ramping the temperature from room temperature to 900 °C at 5 °C min^{-1}.

GC-MS spectrometry was carried out on a HP 6890A spectrometer, with an achiral HP-5 column (0.25 nm × 30 m × 0.25 μm).

Inductively coupled plasma atomic emission spectroscopy (ICP-AES) were performed on a Arcos spectrometer in order to obtain the metal amount in supported nanopartciles. Samples were digested in concentrated nitric acid (10 mg of sample per 2 mL HNO_3) using a Anton Paar microwave. The resulting solutions were transferred to flasks and diluted to 50 mL with water.

Fourier Transform Infrared (FTIR) spectra were obtained using a Bruker Equinox 55 spectrophotometer. The spectra were recorded using a potassium bromide pellets with a resolution of 4 cm^{-1} and 32 scans in the range of 400–4000 cm^{-1}.

Nuclear Magnetic Resonance (NMR) spectra were recorded on a Varian Mercury 400 MHz instrument. Chemical shift values for ^{1}H and ^{13}C were referred to internal $SiMe_4$ (0.0 ppm). Significant peaks are tabulated in the order: multiplicity (**s**, singlet; **d**, doublet; **t**, triplet; **q**, quartet; **m**, multiplet; **br s**, broad singlet), coupling constant(s) in Hertz (Hz) and number of protons. High resolution electrospray mass spectra (HR-ESI) were collected in positive mode on a MAT95XL from Thermo Finnigan. Matrix assisted laser desorption mass spectrometryanalyses were performed on a BrukerBiflex III MALDI-TOF spectrometer using dithranol as matrix. The instrument was equipped with a nitrogen laser emitting at 337 nm, a 2 GHz sampling rate digitizer, a pulsed ion extraction source and are flectron. Fourier transform infrared spectra were recorded in pressed ATR mode on a Bruker Vector 22 spectrometer.

S1.3. General procedure for the partial hydrogenation of alkynes to (*Z*)-alkenes

Autoclave Par 477 equipped with PID control temperature was used as reactor for hydrogenation reactions. In a typical experiment, the autoclave was charged in a glove-box with Ni-NPs@CNTs (17 mg, 3 mmol% of Ni; the catalyst concentration was calculated based on the 10 % of Ni immobilized on the CNTs) and the substrate (1 mmol) in 10 ml of THF. Molecular hydrogen was then introduced until 5 bars of pressure. The reaction was stirred during the corresponding time at 50°C. The autoclave was then depressurized and the resulting solution was filtered over a pad of Celite and analyzed by gas chromatography. The reaction products were analyzed by GC-MS spectrometry. Isolated yields were obtained by flash column chromatography and the products were characterized by ^{1}H and ^{13}C NMR spectroscopy. NMR data of each compound were in agreement with previous reported values.[4-8]

S2. Synthesis of the imidazoliumm carboxilate

The N,N'-dimethyl imidazolium-2-carboxylate (Me_2Im-CO_2) was synthesized by alkylation of methylimidazole with dimethyl carbonate following a reported procedure.[9] Briefly, a screw-top pressure tube was charged with dimethyl carbonate (3.0 mL), 1-methylimidazole (2 mL), and a stir bar. It was sealed and heated for 48 h at 90 °C. The solid was filtered, washed thoroughly with methylene chloride, acetone, and ether and dried under vacuum.

S3. Synthesis of colloidal and CNT-supported Ni nanoparticles

In a typical procedure, $Ni(COD)_2$ (66 mg, 0.24 mmol) and CNTs (127mg) were weighed in a glove and introduced into a Fisher Porter reactor and dissolved in 150 mL of dry and deoxygenated. The imidazolium carboxylate (Me_2Im-CO_2) was separately weighed (0.2, 0.5 or 1.0 equivalents) and introduced into the as-prepared solution. The Fisher Porter reactor was then tightly closed and connected to the argon/vacuum ramp. All tubing was purged under vacuum/argon cycles before the reactor was pressurized with 3 bars $H_{2.}$ Finally, the reactor was placed into an oil bath and the temperature was raised to the desired level (60 ºC). The reaction was left running overnight. A small amount (5 drops approx.) of the resulting dispersion was deposited under an argon atmosphere on a carbon-covered copper grid for transmission electron microscopy analysis (TEM). The rest of the solution was then filtered through a Nylon 66 membrane (Filter-Lab, 0.45 µm × 47 mm), and washed with THF several times. The final product was then dried under vacuum to remove the residual solvent. Unsupported Ni nanoparticles were also obtained following the same methodology.

Commercial CNTs (PR-24-XT-LHT, PYROGRAP®) were used as support. It is important to note that Ni was not detected by ICP for the naked CNTs since they are synthesized from a Fe precursor as growth catalyst (Fe loading < 0.6 wt.% - ICP). Appropriate amounts of metal precursors were used to obtain a theoretical metal loading of 10 wt% onto CNTs

S4. Characterization of the colloidal Ni nanoparticles

TGA.

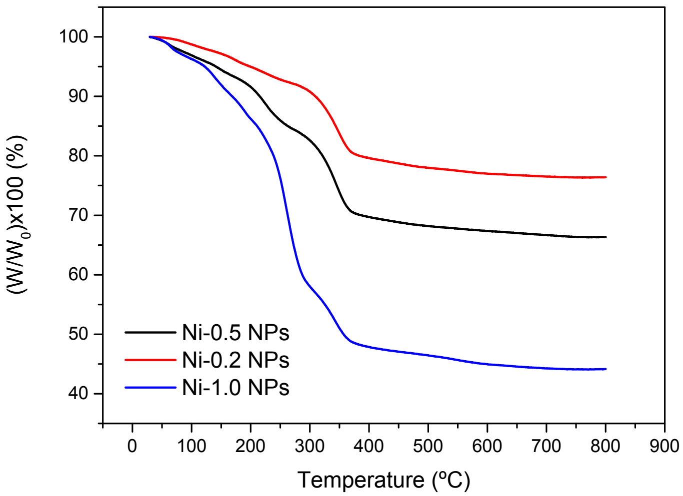

Figure S1. TGA profiles in N_2 of Ni-0.2**,** Ni-0.5 and Ni-1 nanoparticles**.**

From TGA analysis the fraction (wt.%) of the organic part and the metal was obtained for all the samples assuming that the metal content is the residual value at the highest temperature (900 ºC).

Ni-0.5 NPs: 27.4 wt.% of organic part (free NHC), 66.3 wt.% of Ni.

Ni-0.2 NPs: 14.8 wt.% of organic part (free NHC), 76.4 wt.% of Ni.

Ni-1.0 NPs: 44.0 wt.% of organic part (free NHC), 44.1 wt.% of Ni.

HR-TEM

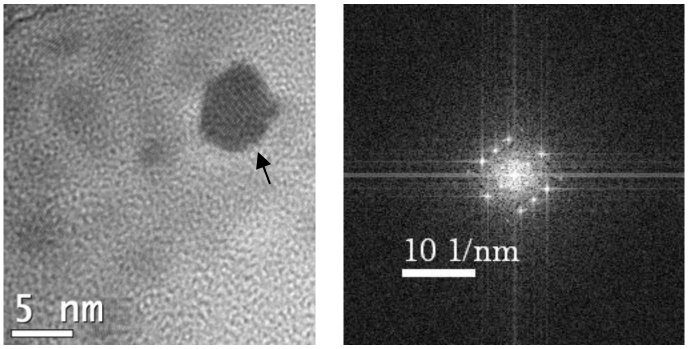

Figure S2. HR-TEM micrograph and electron diffracion patern of Ni-0.5 NPs.

XRD

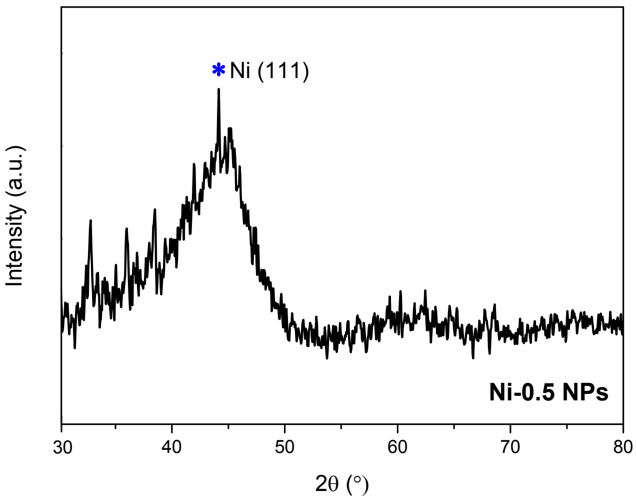

Figure S3. XRD pattern of Ni-0.5 NPs.

Fcc crystalline Ni nanoparticles. Crystal size Ni = 1.2 nm

XPS

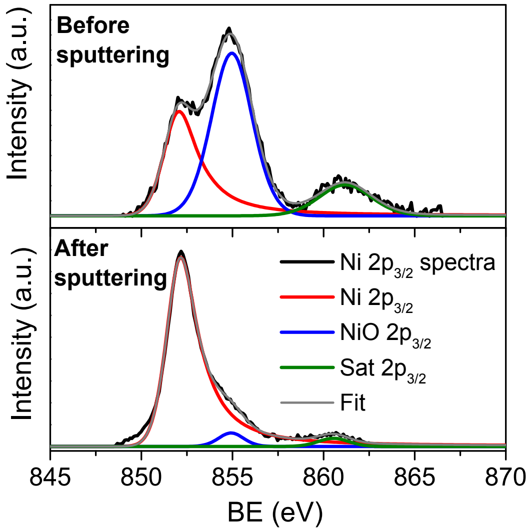

Figure S4. Ni 2p spectra of Ni-0.5 NPs, before and after Ar sputtering.

Table S1. Ni and NiO atomic content from the deconvolution of the Ni2p$_{3/2}$ spectra for colloidal Ni-0.5 NPs.

Sample	**Ni (at.%)**	**NiO (at.%)**
Ni-0.5 NPs. Before Ar sputtering	32.4	67.6
Ni-0.5 NPs. After Ar sputtering	95.5	4.5

S5. Validation of the procedure

TEM

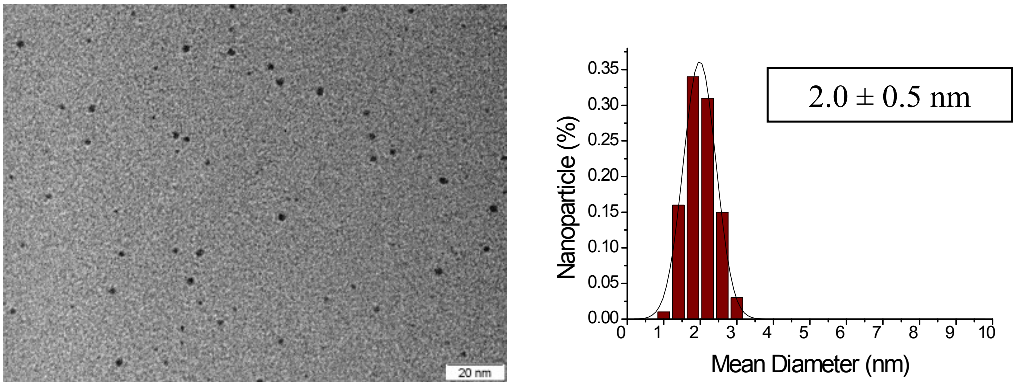

Figure S5. TEM micrograph and size distribution of the Ni-0.5 NPs by the “in-situ” methodology.

IR

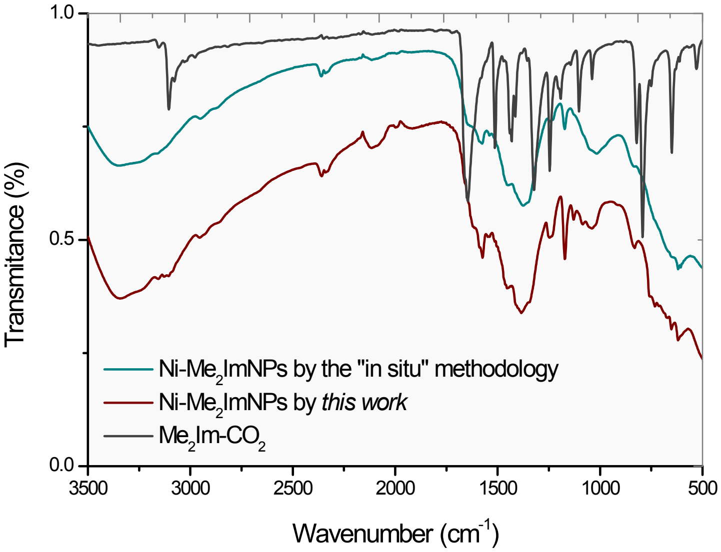

Figure S6. IR spectra of Ni-Me$_2$ImNPs prepared by deprotonation of an imidazolium salt with KOtBu (blue), Ni-Me$_2$ImNPs prepared by in situ decarboxylation of **Me$_2$Im-CO$_2$** (red) and of the imidazolium carboxylate salt **Me$_2$ImCO$_2$** (grey).

TGA

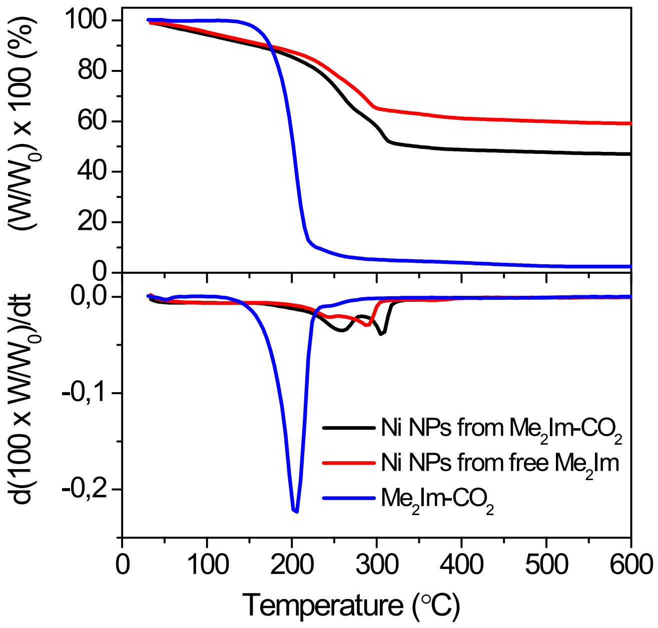

Figure S7. TGA profiles in air, weight percentage and mass variation velocity as a function of the temperature of nickel nanoparticles obtained from the imidazolium carboxylate salt (black curves) and the free NHC (red curves) and of the zwitterionic salt (blue curves, Me_2Im-CO_2).

Ni-0.5 NPs: 52.7 wt.% of organic part (free NHC), 45.6 wt.% of Ni.

Ni-0.5 NPs by the “in-situ” methodology: 42.0 wt.% of organic part (free NHC), 57.3 wt.% of Ni.

S6. Characterization of the CNT-supported Ni nanoparticles

STEM

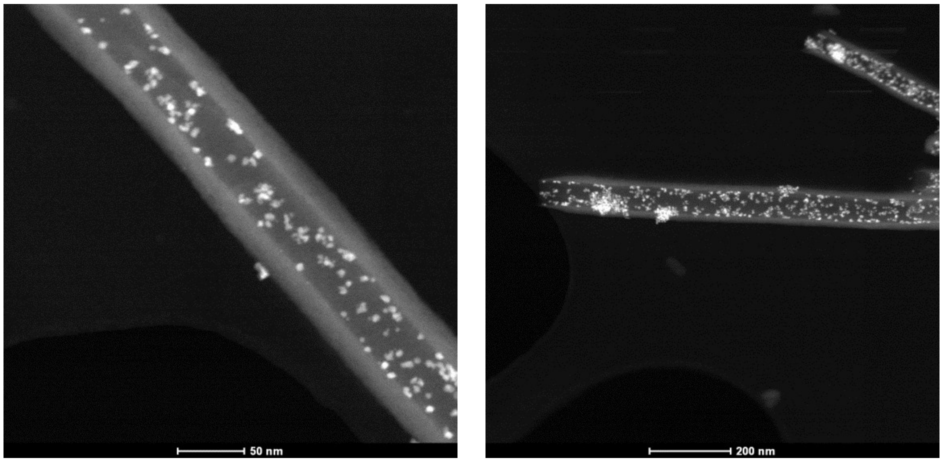

Figure S8. STEM micrographs of Ni-0.5 NPs@CNTs.

HR-TEM

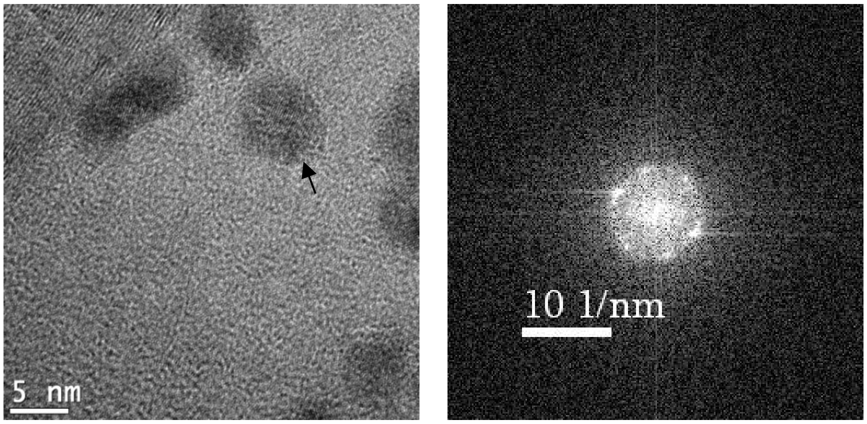

Figure S9. HR-TEM micrographs and electron diffracion patern of Ni-0.5 NPs@CNTs.

TGA

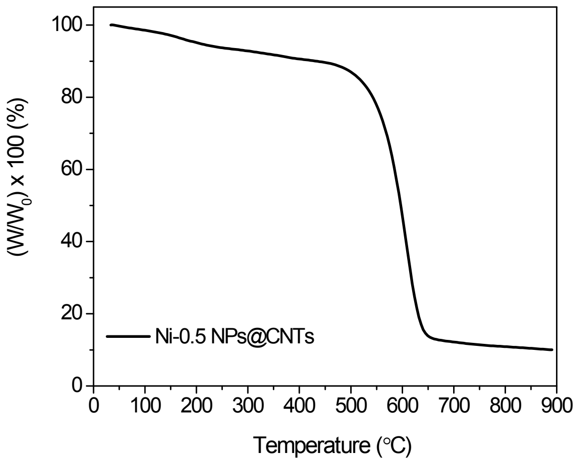

Figure S10. TGA profile in air of Ni-0.5 NPs@CNTs.

Ni-0.5 NPs@CNTs: 10.0 % wt. of Ni.

XRD

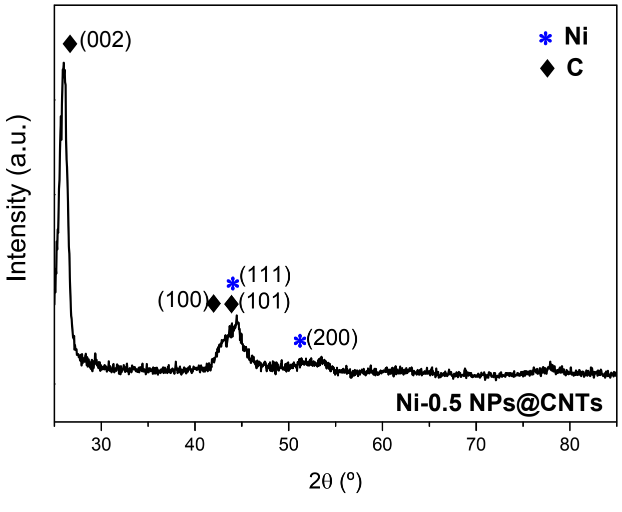

Figure S11. XRD pattern of Ni-0.5 NPs@CNTs.

Fcc crystalline Ni nanoparticles. Crystal size Ni = 2.3 nm

XPS

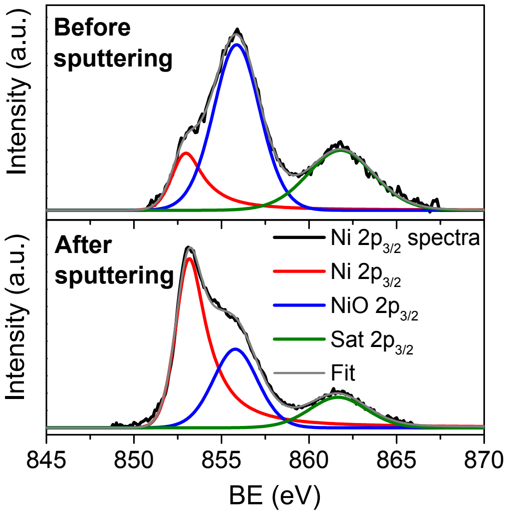

Figure S12. Ni 2p spectra of Ni-0.5 NPs@CNTs, before and after Ar sputtering.

Table S2. Ni and NiO atomic content from the deconvolution of the Ni2$p_{3/2}$ spectra for colloidal and supported nickel nanoparticles.

Sample	Ni (at.%)	NiO (at.%)
Ni-0.5 NPs@CNTs. Before Ar sputtering	17.1	82.9
Ni-0.5 NPs@CNTs. After Ar sputtering	72.7	27.3

Table S3. C, O and Ni content (wt.%) obtained from XPS for colloidal and supported nickel nanoparticles.

Sample	C (wt.%)	O (wt.%)	Ni (wt.%)
Ni-0.5 NPs@CNTs. Before Ar sputtering	90.6	4.6	4.8
Ni-0.5 NPs@CNTs.	90.0	3.8	6.2

After Ar sputtering			

S6. References

(1) Langford, J. I.; Wilson, A. J. C. *J. Appl. Crystallogr.* **1978**, *11*, 102.

(2) Grosvenor, A. P.; Biesinger, M. C.; Smart, R. S. C.; McIntyre, N. S. *Surface Science* **2006**, *600*, 1771.

(3) Biesinger, M. C.; Payne, B. P.; Lau, L. W. M.; Gerson, A.; Smart, R. S. C. *Surf. Interface Anal.* **2009**, *41*, 324.

(4) Belger, C.; Neisius, N. M.; Plietker, B. Chem. Eur. J. **2010**, 16, 12214-12220.

(5) Hori, J.; Murata, K.; Sugai, T.; Shinohara, H.; Noyori, R.; Arai, N.; Kurono, N.; Ohkuma, T. Adv. Synth. Catal. **2009**, 351, 3143-3149.

(6) Pavlakos, E.; Georgiou, T.; Tofi, M.; Montagnon, T.; Vassilikogiannakis, G. *Org. Lett.* **2009**, *11*, 4556-4559.

(7) Moussaoui, Y.; Said, K.; Ben Salem, R. *Arkivoc*, **2006**, 1-22.

(8) Riveiros, R.; Saya, L.; Sestelo, J. P.; Sarandeses, L. A. *Eur. J. Org. Chem.* **2008**, 1959-1966.

(9) Voutchkova, A. M.; Feliz, M.; Clot, E.; Eisenstein, O.; Crabtree, R. H. *J. Am. Chem. Soc.* **2007**, *129*, 12834.